Photovoltage in nanocrystalline porous TiO_2

V. Duzhko, V. Yu. Timoshenko,* F. Koch, and Th. Dittrich
Technische Universität München, Physik Department E16, D-85748 Garching, Germany
(Received 7 August 2000; revised manuscript received 1 March 2001; published 26 July 2001)

Transient and spectral photovoltage (PV) is investigated in nanocrystalline porous TiO_2, which belongs to a class of materials with a very low electrical conductivity, i.e., with a huge Maxwell relaxation time. The PV in such materials is caused by diffusion of excess charge carriers with different diffusion coefficients. Usually, the diffusion coefficient for electrons is larger than that for holes in porous TiO_2. The PV transients are strongly retarded in time with respect to the exciting light pulse. The retardation of the photovoltage transients becomes stronger with decreasing size of the interconnected TiO_2 nanoparticles and generation of defect states. The band gap of porous TiO_2 (rutile, anatase) and the preferential formation of electron traps below the band gap are analyzed.

DOI: 10.1103/PhysRevB.64.075204 PACS number(s): 73.50.Pz, 72.40.+w

I. INTRODUCTION

A photovoltage (PV) arises whenever light induced excess charge carriers are separated in space. Therefore, the formation of a PV signal is determined by the fundamental properties of light absorption and transport of excess carriers in a semiconducting material. PV spectroscopy and transient PV can be used not only for characterization of new materials but also for getting new insights into the mechanism of formation of PV signals in nonconventional semiconductors.

Semiconductors can be divided into materials with a very low or a very high Maxwell relaxation time ($\tau_M = \varepsilon\varepsilon_0/\sigma$, where ε is dielectric constant, $\varepsilon_0 = 8.85 \cdot 10^{-12}$ As/Vm, and σ is electrical conductivity) with respect to the time of measurements. Conventional semiconductors (high mobility, relatively high free-carrier concentration) are characterized by very low values of τ_M while τ_M is huge for some new classes of semiconducting materials as semiconducting polymers, porous semiconductors and dielectrics, or metal oxides as ferroelectrics. The big differences in τ_M cause different mechanisms of PV formation. The surface PV (screening of the built-in electric field by excess carriers)[1] or so-called Dember PV (due to ambipolar diffusion with different diffusion coefficients for excess electrons and holes)[2] are well known for conventional semiconductors. The motion of excess electrons and holes can be considered as diffusion which is *independent* from each other for times $t \ll \tau_M$. This leads, if the diffusion coefficients for excess electrons and holes are different, to the formation of the so-called diffusion PV. Recently, we demonstrated some common features of transient diffusion PV in poly(p-phenylene vinylene)[3] and porous semiconductors.[4] Kronik *et al.* showed by contact potential difference measurements the importance of diffusion-like transport for the formation of the PV in CdSe quantum dot films.[5]

Porous TiO_2 belongs to the class of materials with very low values of σ.[6] Porous TiO_2 is characterized by the complicated structure of a sintered network of TiO_2 nanoparticles and by an enormous internal surface area.[7] The optical band gap (E_G) of TiO_2 is 3.06 eV,[8] (rutile) and 3.2–3.7 eV Refs. 9–11 (anatase, depending on the preparation and measurement conditions). The surface of porous TiO_2 can be easily conditioned by changing the gas ambience. The diffusion coefficient of excess electrons has been obtained from transient photocurrent measurements on porous TiO_2 immersed in electrolyte.[12] The electron drift mobility in porous TiO_2,[13] is 5–6 orders of magnitude lower than the electron Hall mobility in TiO_2 (rutile,[14] anatase[15]) and σ depends strongly on the partial pressure of oxygen.[6] However, the basic mechanisms limiting the electrical transport in porous semiconductors are not well understood up to now.

In this work we develop and apply the concept of diffusion PV to the problem of optical absorption, electronic surface states and transport of excess carriers of charge in nanocrystalline porous TiO_2 layers.

II. SAMPLES

Different pastes containing TiO_2 nanocrystals of anatase or rutile (INAP GmbH) are used for the preparation of porous TiO_2 layers. The glass substrate is covered with a transparent conducting SnO_2:F layer. The porous TiO_2 layers are prepared by screen printing of the paste on the substrate and subsequent firing at 450 °C in air for 30 mins. The thickness of the TiO_2 layer is typically $d = 4\,\mu$m for the samples used in the PV experiments. Some control experiments are carried out on samples with d from 1 to 12 μm and on different substrates (glass without SnO_2:F or mica).

The TiO_2 nanoparticles of different samples are characterized by Raman scattering and x-ray diffraction [Fig. 1(a) and 1(b), respectively]. Characteristic modes appear in the Raman spectra at 143 cm^{-1} (B_{1g}), 447 cm^{-1} (E_g), and 612 cm^{-1} (A_{1g}), which are well known for crystalline rutile,[16] and at 145 and 640 cm^{-1} (E_g), 399 cm^{-1} ($B1_g$), 516 cm^{-1} (doublet A_{1g} and B_{1_g}), which are assigned to the anatase phase of TiO_2.[17] The third E_g mode at 198 cm^{-1}, which is well resolved for anatase single crystals as a small narrow peak[18] is seen only slightly for the porous TiO_2 layer of anatase (16 nm) but not for the porous TiO_2 layer of anatase (6 nm). The mode at 198 cm^{-1} disappears also for anodic nanoporous layers of anatase for which disorder is important.[19] As can be seen from Fig. 1 the porous TiO_2 layers contain nanoparticles of only one crystalline phase. The average size (L) of the nanocrystals is determined from

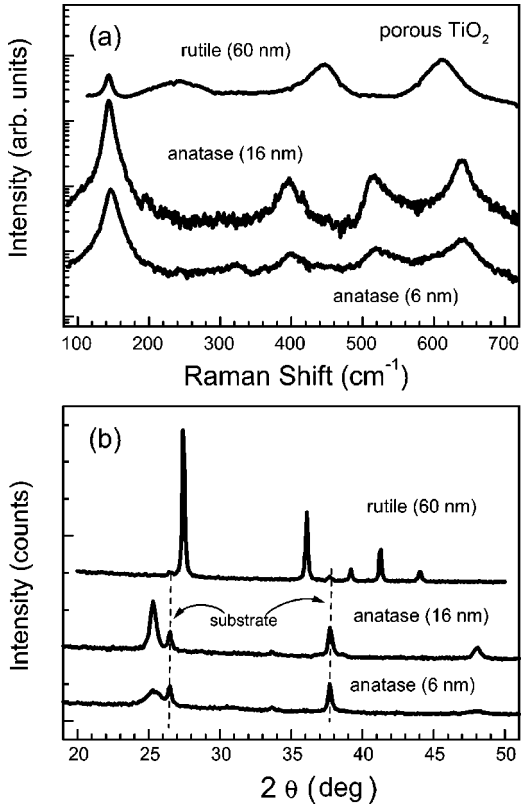

FIG. 1. Raman spectra (a) and x-ray diffraction angle dependence (b) for porous TiO_2 layers of rutile (60 nm), anatase (16 nm), and anatase (6 nm).

the broadening of the peaks in the angular x-ray diffraction dependence [Fig. 1(b)], using the Debeye-Scherrer equation $L=0.9(\lambda/\cos\theta\cdot\Delta\theta)$, where $\lambda=0.154$ nm (Cu K_α line), θ is the Bragg angle, and $\Delta\theta$ is the full width of peak at the half maximum.[20] On the basis of this analysis the porous TiO_2 layers of rutile with diameter of crystallites of 60 nm and of anatase with diameters of crystallites of 16 and 6 nm are distinguished. These layers are used in the PV experiments and denoted as rutile (60 nm), anatase (16 nm) and anatase (6 nm), respectively.

The porous TiO_2 layers are investigated in a vacuum chamber specially designed for the PV measurements. The as prepared samples (just after the annealing in air at 450 °C) are considered as ''well passivated,'' i.e., with low defect density, as will be shown below. The porous TiO_2 layers stored in vacuum are characterized by losses of oxygen and/or water at the surface of TiO_2 nanocrystals. Therefore, these samples were used to investigate the role of defects in the PV formation.

III. PHOTOVOLTAGE MEASUREMENTS

The PV measurements were carried out in the fixed parallel-plate capacitor arrangement that consists of the porous TiO_2 layer on the substrate with SnO_2:F, a 10-μm-thick mica spacer and a semitransparent Cr-electrode evaporated on a quartz homogenizer (Fig. 2). The diameter of the capacitor is 5 mm. This arrangement has the advantage, in

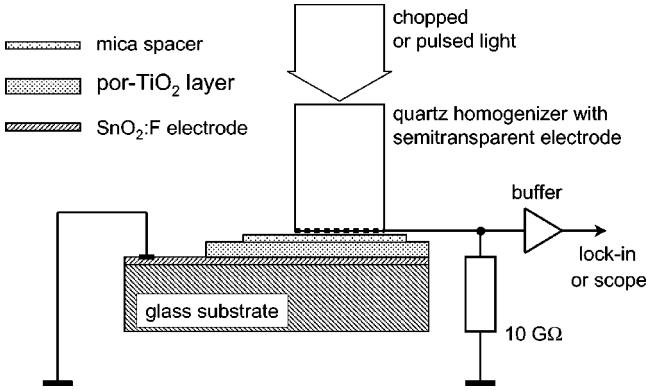

FIG. 2. Experimental setup for the photovoltage measurements.

comparison to PV measurements with a Kelvin probe, that the investigation of transient PV is performed on the time scale between 1 ns and 0.1 s. The time resolution is limited to the short times by the high-impedance buffer (900 MHz) and by the oscilloscope (HP 54520A, 500 MHz). Charging of the capacitor via the high resistance limits the measurements to times less than $RC=0.01-0.1$ s.

A 1000 W Xe lamp with a quartz-prism monochromator was used to excite the spectral dependent PV in the range of 1–4 eV. The light was chopped with the frequency of 20–70 Hz. A N_2 laser (photon energy $h\nu=3.7$ eV, duration time of a pulse 0.5 ns, maximal energy density per pulse about 500 μJ/cm^2) with a dye laser ($h\nu=2.8$ eV) was used for the excitation of PV transients. The SnO_2:F electrode served as a reference electrode.

The PV spectra were measured by a lock-in amplifier as the cophased and phase shifted by $\pi/2$ photovoltage signals (U_x and U_y signals, respectively) with respect to the chopped light. A sample of *n*-type crystalline Si was used for the calibration of initial phase of lock-in amplifier. The PV transient of this sample has a positive sign (excess electrons move toward the bulk and excess holes move toward the surface in the electric field of surface space-charge region), reaches the maximum value within the duration of laser pulse and drops almost to zero in microsecond range. For c-Si the PV spectra with respect to the illumination by lamp (chopping frequency 70 Hz) have a positive U_x signal and $U_x \gg U_y$. The U_y-signal characterizes the phase shift between the chopped light and the PV signal. An essential U_y signal points to a slow increase and decrease of the PV signal in comparison to the half period of chopping. Some data are presented as normalized amplitude ($U_{ph}^{amp}/\Phi = \sqrt{U_x^2+U_y^2}/\Phi$) and phase ($\tan\varphi = U_y/U_x$) of the PV signal. The PV spectra are measured in the regime of weak excitation when U_{ph}^{amp} depends linearly on the photon flux Φ (excitation intensity divided by $h\nu$).

IV. RESULTS AND DISCUSSION

A. Transient photovoltage in well-passivated porous TiO_2 layers

Figure 3 shows PV transients for porous TiO_2 layers of rutile (60 nm), anatase (16 nm), and anatase (6 nm) in air.

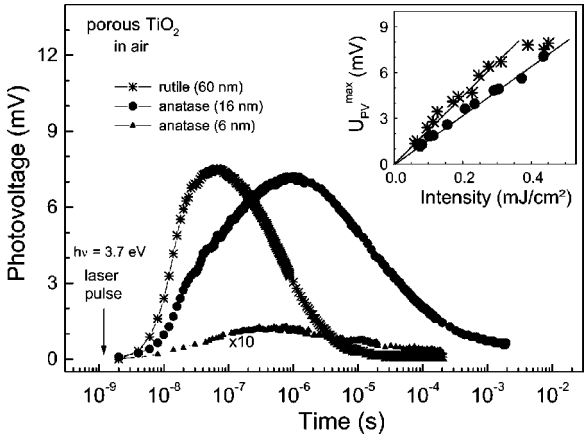

FIG. 3. Photovoltage transients for as prepared porous TiO_2 layers of rutile (60 nm), anatase (16 nm), and anatase (6 nm) in air. Inset: dependence of the maximum of the photovoltage on the excitation intensity for rutile (60 nm) and anatase (16 nm).

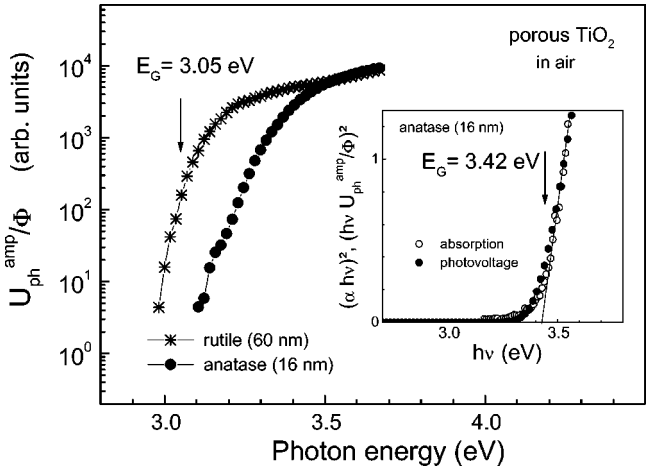

FIG. 4. Spectra of the photovoltage-amplitude normalized to the photon flux (U_{PV}^{amp}/Φ) for as prepared porous TiO_2 layers of rutile (60 nm) and anatase (16 nm) shown in a semilog scale. Inset compares the spectra of squares of $h\nu(U_{PV}^{amp}/\Phi)$ and of $h\nu\alpha$ for an as prepared porous TiO_2 layer of anatase (16 nm).

The excess carriers are excited with photons of $h\nu > E_G$. The sign of the PV transients is positive. The positive sign of the PV implies that the photoexcited electrons move faster than holes towards the porous TiO_2/SnO_2:F interface. No PV signal could be detected for $h\nu < E_G$. The most striking feature of these transients is their retardation in time, i.e., the transient PV signal is roughly zero just after the laser pulse and develops within the following 0.1 μs (rutile) or 1 μs (anatase). The observed retardation of the transient PV differs drastically from the transient PV in crystalline semiconductors that appears immediately with the exciting laser pulse. The built-in electric field induced by the discontinuity of the material at the top of the layer is very weak in porous TiO_2 due to its high porosity, enormous surface area, and negligible concentration of equilibrium charge carriers. The retardation of the transient PV is caused by slow and independent diffusion of excess electrons and holes. The gradient of excess electron and hole concentrations is caused by nonhomogeneous absorption of light with photons of $h\nu > E_G$.

The shape of the PV transients does not depend on the thickness of the porous TiO_2 layers (changes from 1 to 12 μm). Therefore, the diffusion length of excess electrons and holes is much shorter than the thickness of the porous TiO_2 layers. As remark, the PV transients showed two negative extrema in the case of illumination through the semitransparent SnO_2:F back electrode. The first extremum at about 10 ns was related to separation of charge at the porous TiO_2/SnO_2:F interface (injection of excess electrons from porous TiO_2 into SnO_2:F) while the second one (in the μs range) belonged to the diffusion PV. Control experiments showed that the shape of the PV transient was independent of the used substrate in the usual case of illumination from the porous TiO_2 (front) side.

The intensity dependence of the PV signal in the maximum of the transients (U_{PV}^{max}) is given in the inset of Fig. 3. This dependence is linear up to 0.3 mJ/cm^2 and tends to saturate for the rutile sample at higher intensities. The saturation of U_{PV}^{max} at high excitation intensity can be explained by a nonlinear increase of recombination losses (Auger recombination and bimolecular radiative recombination) with increasing excess carrier concentration. A linear dependence of U_{PV}^{max} on the intensity of the exciting laser pulse is expected for diffusion PV whereas for the Dember PV, a logarithmic dependence would be expected. We remark that a linear intensity dependence takes also place for surface PV in crystalline semiconductors at very low intensity when the excess carrier concentration is much smaller than the equilibrium-carrier concentration. This is not the case in our pulsed PV experiments.

The increasing part of the diffusion PV transient $[U_{diff}(t)]$ in porous TiO_2 layers can be simulated by solving the one-dimensional diffusion equation for nonequilibrium carriers of charge with different diffusion coefficients of electrons (D_e) and holes (D_h) and subsequent integration of the electric field over the thickness of the sample:

$$U_{diff}(t) = \frac{e}{\varepsilon\varepsilon_0}\int_0^d\int_0^x [p(\xi,t) - n(\xi,t)]\,d\xi\,dx, \qquad (1)$$

where $n(\xi,t)$ and $p(\xi,t)$ are the concentrations of nonequilibrium (photoexcited) electrons and holes, respectively, $e = 1.6\times10^{-19}$ As and ε is the effective dielectric constant of the porous layer. The values of $n(\xi,t)$ and $p(\xi,t)$ depend on the excitation intensity, carriers recombination, trapping, and diffusion. However the details of these process are not known for porous TiO_2.

B. Spectral photovoltage in well-passivated porous TiO_2 layers

Spectra of the PV amplitude as prepared for porous TiO_2 layers of rutile (60 nm) and anatase (16 nm) in air are shown in a semilog scale in Fig. 4. The inset compares the spectral dependence of $(\alpha h\nu)^2$, where α and $h\nu$ are the absorption coefficient and the photon energy, respectively, with U_{ph}^{amp}/Φ for the porous TiO_2 layer of anatase (16 nm). The absorption coefficient was obtained from the measurements of optical transmittance of the porous TiO_2 layer on thin glass sub-

strate. The PV data shown in the inset of Fig. 4 are multiplied with a constant to show them simultaneously with the absorption coefficient. The PV amplitude increases strongly in the region of the forbidden gap. The values of the optical gap for rutile and anatase single crystals (3.05 eV Ref. 8 and 3.42 eV Ref. 9, respectively) are in good agreement with the spectral PV measurements. The PV spectrum of the porous anatase contains a pronounced exponential tail, which is practically absent for the porous rutile. The energy of the exponential tail of the PV spectrum of the porous anatase is about 50 meV, what is larger than the Urbach energy of the exponential absorption tails in anatase single crystals (about 40 meV at room temperature[9]). For comparison, the width of Urbach tails is of the order of 78 meV for size of nanoparticles of 4–8 nm in dense layers of anatase (photoconductivity measurements)[21] and 65 meV for hydrogenated amorphous silicon at room temperature (absorption measurements).[22] Therefore, disorder is important in anatase nanocrystals.

We remark that a plot of $(\alpha h\nu)^{1/2}$ (indirect transitions) would give a value of E_G close to 3.2 eV that was also sometimes reported as the band gap of anatase.[23] However, the conclusion that nanoporous anatase has direct or indirect gap cannot be strictly drawn since the approach of the plot of $(\alpha h\nu)^2$ is also conventional for amorphous semiconductors for which the momentum-conservation rule is not strongly held.[24] The plot of $(\alpha h\nu)^2$ vs $h\nu$ was also used successfully for the analysis of the optical absorption of thin anatase layers prepared by spray pyrolysis for which E_G ranges between 3.56 and 3.75 eV.[10]

As shown above, in the spectral range from 3 to 3.5 eV, the amplitude of the PV signal of prepared porous TiO_2 layers follows the absorption coefficient. Taking into account the linear dependence of the PV signal on the excitation light intensity, this fact, can be explained by a mechanism of the PV formation depending on the concentration gradient of excess carriers. According to our measurements of transmittance in the porous TiO_2 layer of anatase (16 nm), the absorption coefficient is of the order of 10^5 cm^{-1}, i.e., the most part of the light is absorbed in the porous TiO_2 layer of depth $d=4$ μm. Therefore the PV signal arises due to the concentration gradient of excess carriers in the porous layer. This makes the spectral PV suitable for the investigation of optical absorption in the case when only one mechanism of the formation of the PV signal is involved.

C. Spectral photovoltage in porous TiO_2 layers with gap states

Figure 5 compares spectra of the U_x and U_y signals for anatase (16 nm) in air (a) or under vacuum condition at 0.05 (b) and 0.001 (c) mbar. The appearance of the U_x signal [Fig. 5(a)] at 3.3 eV is consistent with the band gap of anatase and the presence of tail states below the band gap. The disappearance of the U_x signal at 3.7 eV is not caused simply by the spectrum of the lamp but shows that charge separation is much less effective than recombination for strong absorption. The tails below E_G are much more pronounced for the U_y than for the U_x signal showing that trapping of charge into electronic states in the forbidden gap contributes mostly to the retardation of the PV.

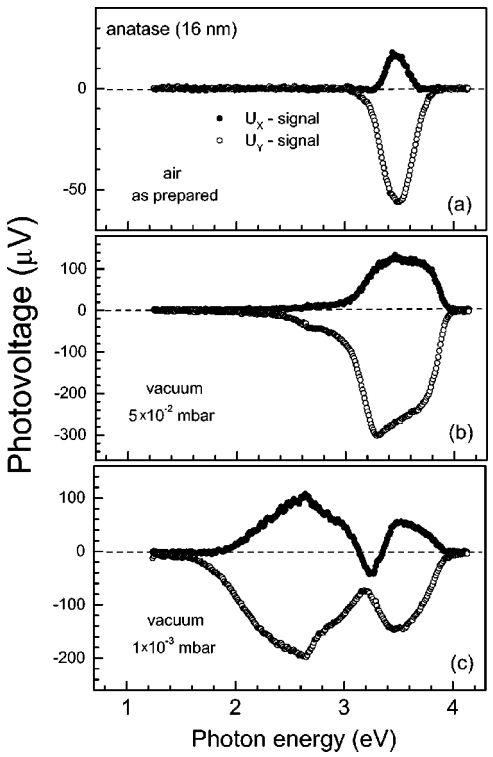

FIG. 5. Photovoltage spectra for as prepared porous TiO_2 layer of anatase (16 nm) in air (a) and in vacuum at 0.05 (b) and 0.001 (c) mbar. The spectra are measured for the *x* and *y* signals at the lock-in amplifier.

The U_x signal at $h\nu=3.5$ eV increases by about six times after keeping the sample in vacuum at $p=5\times10^{-2}$ mbar [Fig. 5(b)]. Further, the spectral range of the U_x signal for the sample kept at $p=5\times10^{-2}$ mbar is extended to lower and higher photon energies giving evidence, respectively, for generation of defect states in the forbidden gap and for more efficient charge separation in the case of strong absorption. Hence, the generation of electronic states below E_G can sufficiently enhance the charge separation.

The U_x signal for the layer of anatase (16 nm) at $h\nu=3.5$ eV decreases twice in comparison to $p=5\times10^{-2}$ mbar after keeping the sample at $p=10^{-3}$ mbar [Fig. 5(c)] and the PV spectrum is dominated by a huge defect peak with maximum at 2.7 eV. Therefore, the concentration of electronic states below E_G increases strongly and the distribution of defect states broadens out with decreasing pressure. The U_x signal drops sharply and changes in the spectral range from 3 to 3.5 eV. The U_y signal arises at 1.5 eV and follows mainly the mirrored shape of the U_x signal but without changing the sign. We remark that the PV spectra are further changing during prolonged storage in vacuum showing that a long time is necessary to reach a chemical equilibrium between formation and annihilation of defect states at the surface of TiO_2.

The change of the sign of the U_x signal from positive to negative is caused by the change of the diffusion coefficients

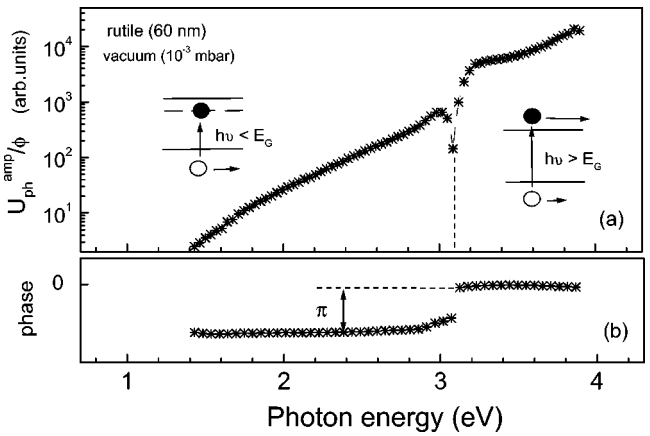

FIG. 6. Spectra of the photovoltage-amplitude normalized to the photon flux (a) and of the phase of the photovoltage signal (b) for porous TiO_2 layers of rutile (60 nm) in a semilog scale under vacuum condition (0.001 mbar). The inset depicts the formation of the PV signal for $h\nu < E_G$ (left side) and for $h\nu > E_G$ (right side) .

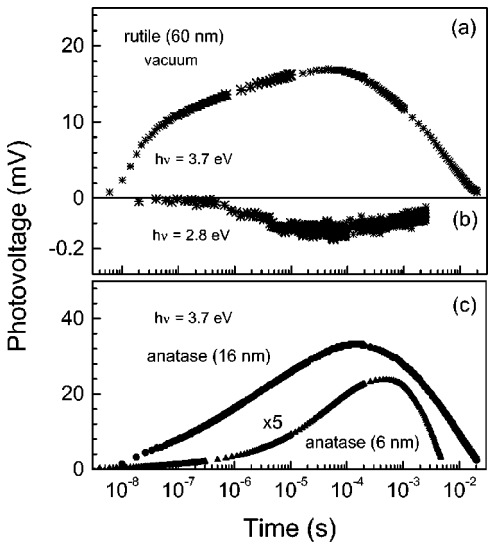

FIG. 7. Photovoltage transients for porous TiO_2 layers of rutile (60 nm), anatase (16 nm), and anatase (6 nm) under vacuum condition (0.001 mbar). The excitation of excess carriers of charge was performed with $h\nu = 3.7$ eV (a, c) and $h\nu = 2.8$ eV (b).

from $D_e > D_h$ to $D_e < D_h$. A change of the sign of the PV signal for the whole range of $h\nu < E_G$ could be realized for the layers of porous TiO_2 (rutile) and porous TiO_2 (anatase, 6 nm) under vacuum condition. Figure 6 shows the spectra of U_{ph}^{amp}/Φ and of the phase for the layer of porous TiO_2 (rutile) in vacuum (0.001 mbar). The defect formation in the porous anatase is stronger than for the porous rutile and this process is even accompanied by formation of well-defined defect band in the spectral range from 3 to 3.4 eV. The more efficient defect formation in the porous anatase is probably related to the smaller size of nanocrystals (larger internal surface area). Another possible reason for the defect formation in porous anatase is weaker bonding of oxygen in an elementary octahedron of that phase of TiO_2.[17]

The discontinuity of the phase is located at the position of the band gap for the porous-TiO_2 layer of rutile (60 nm) in vacuum. This means that electrons or holes are accelerated toward the back electrode for $h\nu > E_G$ or for $h\nu < E_G$, respectively. This means that electron traps are preferentially generated in porous TiO_2 (rutile) under vacuum condition (see inset of Fig. 6). It can be further concluded, with respect to the PV amplitudes, that the diffusion coefficient of excess holes moving in the valence band is lower but not much lower than that for excess electrons moving in the conduction band. The phase is shifted by π at 3.6 eV for the porous-TiO_2 layer of anatase (6 nm). This blue shift of E_G by about 150 meV in comparison to E_G for anatase (16 nm) is caused by the quantum confinement effect[25] and was also observed by absorption and photoluminescence measurements on TiO_2 nanoparticles used for catalytic reactions.[26] We remark that the photon energy at which the sign of the PV signal changes marks the mobility gap for the electrons.

The loss of oxygen leads to the formation of donor states in reduced TiO_2.[27] For rutile single crystals a peak with maximum position of about 0.7 eV below the conduction-band edge was measured by photoelectron spectroscopy on reduced rutile and assigned to oxygen vacancies.[28] The position of the energy levels of the corresponding defect states in porous TiO_2 stored in vacuum is expected to be in the same order of magnitude (some 100 meV below the conduction band). These states should be considered, in our opinion, as electron traps leading to a change of PV for $h\nu < E_G$. The PV signal at $h\nu < E_G$ practically vanished after adsorption of water molecules that demonstrated the role of water for the passivation of electron-surface traps. However, prolonged storage of porous TiO_2 in vacuum caused nonreversible defect formation in the sample for which the PV signal at $h\nu < E_G$ did not vanish after adsorption of water molecules. They could be removed only by thermal annealing in air at temperatures higher than 400 °C. Further heavily reduced TiO_2 crystals are dark.[29] Therefore, the formation of donor states is accompanied by the formation of deep defect states acting also as recombination centers.

D. Transient photovoltage in porous TiO_2 layers with gap states

Photovoltage transients are shown in Fig. 7 for porous-TiO_2 layers of rutile (60 nm), anatase (16 nm), and anatase (6 nm) with electron traps induced by the storage of the samples in vacuum. The excitation of excess carriers of charge is performed with $h\nu > E_G$ [(a) and (c), $h\nu = 3.7$ eV] and $h\nu < E_G$ [(b), $h\nu = 2.8$ eV]. The sign of the transient PV is positive for $h\nu > E_G$ and negative for $h\nu < E_G$. This is consistent with the spectral PV measurements. The transient PV signal is much lower for the excitation with $h\nu < E_G$ than for the excitation with $h\nu > E_G$. This is not surprising because the spectral PV signal at $h\nu = 2.8$ eV is lower than the spectral PV signal at $h\nu = 3.7$ eV by more than one order of magnitude.

The retardation behavior of the PV transients changes dramatically after generation of gap states. The time of the maximum PV stored in the vacuum sample increases by

about three orders of magnitude in comparison to the samples in air. An increase of the value of U_{PV}^{max} is not essential.

The PV transient of the rutile excited with $h\nu > E_G$ shows a pronounced shoulder at the shorter times ($\leqslant 10^{-7}$ s). This part of the transient is similar with the growth part of PV transient in air (compare corresponding curves in Figs. 3 and 7). It means that the PV formation in submicrosecond scale is not sensitive to the defects created in the TiO_2 under vacuum treatment and shows that charge separation can take place also within one nanoparticle of $\alpha^{-1} < d$.

The PV transients do not decay purely by exponent or logarithmic law. A lifetime of charge carriers could be introduced for exponential decay while the recombination of specially separated charge could be used to describe a logarithmic decay.[30] Therefore, we can describe the recombination process as recombination of spatially separated charge taking into account transport process if the parameters of recombination are known. The diffusion length of photoexcited charge carriers is lower than 1 μm that allows to give only an upper limit of D_e below 10^{-5} cm^2/s for the porous anatase. For comparison, with respect to the drift mobility in porous anatase one will get for D_e a value of about 10^{-7} cm^2/s.[13] The value of D_h should be even lower.

The presence of states in the forbidden-gap leads to an increase of the amplitude of spectral PV and to a much stronger retardation of the PV transients. The creation of defects would hardly increase the carrier lifetime. Therefore, the additional strong retardation of the PV transient gives evidence for a decrease of the diffusion coefficients, and the importance of recombination for the decay of PV.

The size of the TiO_2 nanocrystal and the porosity of the sample can influence the formation of different kinds of electronic states. This question was not investigated in detail in our experiments but we suspect that the differences between the different porous TiO_2 samples are caused by the influence of the dimension of the nanocrystals on the defect states in the forbidden gap.

V. CONCLUSIONS

The photovoltage is formed by the *independent* from each other which are in material with a huge Maxwell relaxation time as porous semiconductors and dielectrics, semiconducting polymers or metal oxides. The concept of the so-called diffusion photovoltage has been used to study the fundamental properties of optical absorption and transport of excess carriers of charge in porous TiO_2. The diffusion coefficient is larger for electrons moving in the conduction band than holes moving in the valence band independent of the phase (rutile, anatase), size of the TiO_2 nanoparticles, and surface states. The diffusion of excess holes has been observed for TiO_2 in the case when electron-traps states are dominantly created in the band gap and the energy of the exciting photons is below E_G. The mobility gap can be clearly separated. The PV transient are strongly retarded in time with respect to the exciting laser pulse while the retardation of the PV transients becomes stronger with decreasing size of the interconnected TiO_2 nanoparticles and generation of defect states.

ACKNOWLEDGMENTS

We are very grateful to Y. Shapira, N. Ashkenasy, and to the referee for helpful criticism. The authors are also grateful to H.-E. Porteanu for help with Raman measurements and to H. Schneider for XRD analysis. V.D. and V.Yu.T. thank the Deutsche Forschungsgemeinschaft and the Alexander von Humboldt Foundation, respectively, for financial support.

*Permanent address: M. V. Lomonosov Moscow State University, Physics Department, 119899 Moscow, Russia.

[1] E. O. Johnson, Phys. Rev. **111**, 153 (1958).
[2] G. Garrett and W. H. Brattain, Phys. Rev. **99**, 376 (1955).
[3] V. Duzhko, Th. Dittrich, B. Kamenev, V. Yu. Timoshenko, and W. Brütting, J. Appl. Phys. **89**, 4410 (2001).
[4] V. Yu. Timoshenko, V. Duzhko, and Th. Dittrich, Phys. Status Solidi A **182**, 227 (2000).
[5] L. Kronik, N. Ashkenasy, M. Leibovitch, E. Fefer, Y. Shapira, S. Gorer, and G. Hodes, J. Electrochem. Soc. **145**, 1748 (1998).
[6] Th. Dittrich, J. Weidmann, F. Koch, I. Uhlendorf, and I. Lauermann, Appl. Phys. Lett. **75**, 3980 (1999).
[7] M. K. Nazeeruddin, A. Kay, I. Rodicio, R. Humphry-Baber, E. Müller, P. Liska, N. Vlachopoulos, and M. Grätzel, J. Am. Chem. Soc. **115**, 6382 (1993).
[8] D. C. Cronemeyer, Phys. Rev. **87**, 876 (1952).
[9] H. Tang, F. Levy, H. Berger, and P. E. Schmid, Phys. Rev. B **52**, 7771 (1995).
[10] S. Zhang, Y. F. Zhu, and D. E. Brodie, Thin Solid Films **213**, 265 (1992).
[11] T. Fuyuki and H. Matsunami, Jpn. J. Appl. Phys., Part 1 **25**, 1288 (1986).
[12] A. Solbrand, H. Lindström, H. Rensmo, A. Hagfeldt, and S.-E. Lindquist, J. Phys. Chem. B **101**, 2514 (1997).
[13] Th. Dittrich, E. A. Lebedev, and J. Weidmann, Phys. Status Solidi A **165**, R5 (1998).
[14] R. G. Breckenridge and W. Hosler, Phys. Rev. **91**, 793 (1953).
[15] L. Forro, O. Chauvet, D. Emin, and L. Zuppiroli, J. Appl. Phys. **75**, 633 (1994).
[16] S. P. S. Porto, P. A. Fleury, and T. C. Damen, Phys. Rev. **154**, 522 (1967).
[17] H. Tang, K. Prasad, R. Sanjines, P. E. Schmid, and F. Levy, J. Appl. Phys. **75**, 2042 (1994).
[18] H. Berger, H. Tang, and F. Levy, J. Cryst. Growth **130**, 108 (1993).
[19] J. Rappich, Dissertation A, Freie Universität Berlin, 1989.
[20] A. Guinier, *X-ray Diffraction* (Freeman, San Francisco, 1963), Chap. 5.
[21] R. Könenkamp, Phys. Rev. B **61**, 11 057 (2000).
[22] G. D. Cody, T. Tiedje, B. Abeles, B. Brooks, and Y. Goldstein, Phys. Rev. Lett. **47**, 1480 (1981).
[23] B. O'Regan and M. Grätzel, Nature (London) **353**, 737 (1991).
[24] This question has been discussed for anodic layers of TiO_2 by K. Leitner, J. W. Schultze, and U. Stimming, J. Electrochem. Soc. **133**, 1561 (1986).
[25] L. E. Brus, J. Chem. Phys. **80**, 4403 (1984).

[26] M. Anpo, T. Shima, S. Kodama, and Y. Kubokawa, J. Phys. Chem. **91**, 4305 (1987).
[27] A. von Hippel, J. Kalnajs, and W. B. Westphal, J. Phys. Chem. Solids **23**, 779 (1962).
[28] R. L. Kurtz, R. Stockbauer, T. E. Madey, E. Roman, and J. L. de Segovia, Surf. Sci. **218**, 178 (1989).
[29] S. Zerfoss, R. G. Stokes, and C. H. Moore, J. Chem. Phys. **16**, 1166 (1946).
[30] D. G. Thomas, J. J. Hopfield, and W. M. Augustyniak, Phys. Rev. **140**, A202 (1965).